Biol Blood Marrow Transplant 25 (2019) 2124–2133

Biology of Blood and Marrow Transplantation

journal homepage: www.bbmt.org

Biology

Macrophages Educated with Exosomes from Primed Mesenchymal Stem Cells Treat Acute Radiation Syndrome by Promoting Hematopoietic Recovery

John A. Kink[1], Matthew H. Forsberg[2], Sofiya Reshetylo[1], Soroush Besharat[1], Charlie J. Childs[1], Jessica D. Pederson[1], Annette Gendron-Fitzpatrick[3], Melissa Graham[3], Paul D. Bates[2], Eric G. Schmuck[1], Amish Raval[1], Peiman Hematti[1,4], Christian M. Capitini[2,4,*]

[1] *Department of Medicine, University of Wisconsin School of Medicine and Public Health, Madison, Wisconsin*
[2] *Department of Pediatrics, University of Wisconsin School of Medicine and Public Health, Madison, Wisconsin*
[3] *The Comparative Pathology Laboratory, Research Animal Resource Center, University of Wisconsin, Madison, Wisconsin*
[4] *University of Wisconsin Carbone Cancer Center, Madison, Wisconsin*

Article history:
Received 1 November 2018
Accepted 23 July 2019

Keywords:
Mesenchymal stem cells
Radiation injury
Exosomes
Macrophages
Acute radiation syndrome
Hematopoiesis

A B S T R A C T

In the setting of radiation-induced trauma, exposure to high levels of radiation can cause an acute radiation syndrome (ARS) causing bone marrow (BM) failure, leading to life-threatening infections, anemia, and thrombocytopenia. We have previously shown that human macrophages educated with human mesenchymal stem cells (MSCs) by coculture can significantly enhance survival of mice exposed to lethal irradiation. In this study, we investigated whether exosomes isolated from MSCs could replace direct coculture with MSCs to generate exosome educated macrophages (EEMs). Functionally unique phenotypes were observed by educating macrophages with exosomes from MSCs (EEMs) primed with bacterial lipopolysaccharide (LPS) at different concentrations (LPS-low EEMs or LPS-high EEMs). LPS-high EEMs were significantly more effective than uneducated macrophages, MSCs, EEMs, or LPS-low EEMs in extending survival after lethal ARS in vivo. Moreover, LPS-high EEMs significantly reduced clinical signs of radiation injury and restored hematopoietic tissue in the BM and spleen as determined by complete blood counts and histology. LPS-high EEMs showed significant increases in gene expression of STAT3, secretion of cytokines like IL-10 and IL-15, and production of growth factors like FLT-3L. LPS-EEMs also showed increased phagocytic activity, which may aid with tissue remodeling. LPS-high EEMs have the potential to be an effective cellular therapy for the management of ARS.

INTRODUCTION

Radiation, delivered therapeutically, accidentally, or maliciously during a terrorist attack, can lead to an acute radiation syndrome (ARS) with life-threatening toxicities. High-dose radiation causes damage to highly proliferative cells found in the bone marrow, gastrointestinal tract, and skin [1]. Current standard of care involves supporting victims with antibiotics and transfusions until they can undergo an allogeneic bone marrow transplant (BMT) from a suitable donor. Unfortunately, the entire BMT process can often take weeks to identify and collect cells from a donor and would be difficult to perform on a large scale in the event of a widespread exposure [2]. Moreover, allogeneic BMTs have their own set of complications, including engraftment failure, opportunistic infections, and/or graft-versus-host disease, making them potentially as toxic as ARS itself. Consequently, identification of new therapeutic agents has received priority for treatment of ARS. However, to date, the only approved agents are colony-stimulating factors like granulocyte-colony stimulating factor (G-CSF) and granulocyte-macrophage colony-stimulating factor (GM-CSF) [3,4]. Unfortunately, these factors require the patient's own hematopoietic stem cells to be effective [5] and do not address restoration of other critical hematopoietic cells, including lymphocytes, erythrocytes, and platelets.

"Off-the-shelf" cell-based therapies are attractive alternatives for repair of tissue injuries after ARS. Ideally, such cell-based therapies could be cryopreserved and then thawed for infusion after radiation exposure. Theoretically, because the patient is already immunosuppressed by radiation, the cell product should not require extensive tissue matching to the recipient. Among the cells actively explored for ARS are mesenchymal stem cells (MSCs) derived from the bone marrow

Financial disclosure: See Acknowledgments on page 2132.
* Correspondence and reprint requests: Christian Capitini, MD, University of Wisconsin, 1111 Highland Avenue, WIMR 4137, Madison, WI 53705.
E-mail address: ccapitini@pediatrics.wisc.edu (C.M. Capitini).

https://doi.org/10.1016/j.bbmt.2019.07.026
1083-8791/

(BM) [4,6]. MSCs are capable of self-renewal and differentiation into osteocytes, chondrocytes, and adipocytes [7]. MSCs have robust immunomodulatory and anti-inflammatory properties, as well as paracrine effects conductive to tissue regeneration [8]. Although the use of MSCs has shown promise in preclinical rodent models of radiation injury [9-13], the lack of consistent cell engraftment indicates that MSCs may achieve their therapeutic effects via communication with other effector cells. Despite strong preclinical potential of MSCs, they have not yet been approved to treat ARS.

We have previously reported that cocultivation of human macrophages with human MSCs generates MSC-educated macrophages (MEMs) [14] capable of prolonging survival in a lethal radiation injury xenogeneic model [15]. Transwell studies indicated that secreted factors from MSCs were involved in alternatively activating macrophages to MEMs, although not to the same degree as direct coculture [14]. Recent studies have shown that a major mode of cell-to-cell communication by MSCs involves the secretion of membrane-bound extracellular vesicles (EVs) [16,17]. In addition, MSCs can shift to either a pro- or anti-inflammatory phenotype through the activation of surface Toll-like receptors by products released from pathogens such as lipopolysaccharide (LPS) or from damaged tissue via poly I:C [18]. In this study, we hypothesized that EVs could replace the need for MSC coculture and educate macrophages to become radioprotective.

Here we determined, based on vesicle size, that EVs produced from unprimed or LPS-primed MSCs consisted largely of exosomes. We used exosomes from unprimed MSCs to produce exosome-educated macrophages (EEMs) or exosomes from MSCs primed with 2 different doses of LPS to produce EEMs (LPS-low or LPS-high EEMs). We found that LPS-high EEMs improved survival from lethal radiation injury in mice compared with vehicle, MSCs, macrophages, EEMs, and LPS-low EEMs. The protective effects by LPS-high EEMs were due to restored hematopoietic tissue in the spleen and bone marrow, in part through secretion of cytokines and growth factors as well as increased phagocytic activity, which is needed for tissue remodeling.

MATERIALS AND METHODS

Macrophage Generation

Human peripheral blood mononuclear cells were collected by density gradient separation using Ficoll-Paque Plus (endotoxin tested) (GE Healthcare Bio-Sciences, Piscataway, NJ) from healthy stem cell donors using an institutional review board-approved protocol. RBCs were lysed by incubating cells in ACK lysis buffer (Lonza, Walkersville, MD) for 3 minutes. To reduce platelet contamination, cell suspensions were centrifuged at 300 to 700 rpm for 10 minutes and cell pellets were resuspended and incubated with anti-human CD14 microbeads (Miltenyi Biotec, Auburn, CA) for 15 minutes at 4°C. After washing unbound antibody, cell separation was done using an autoMACS Pro Separator (Miltenyi Biotec). Purified $CD14^+$ monocytes were plated into 6-well cell culture plates at a concentration of 0.5 to 1×10^6 per well for in vitro studies or 10^7 per T75 cm^2 filter cap cell culture flask for in vivo studies (Greiner Bio-One, Monroe, NC) in Iscove's modified Dulbecco's media (Gibco, Life Technologies, Grand Island, NY) supplemented with 10% human serum blood type AB (Mediatech, Herndon, VA), 1× nonessential amino acids (Lonza, Walkersville, MD), 4 mM L-glutamine (Invitrogen, Carlsbad, CA), 1 mM sodium pyruvate (Mediatech), and 4 μg/mL recombinant human insulin (Invitrogen). Monocytes were cultured for 7 days at 37°C with 5% CO_2, without cytokines, to allow differentiation to macrophages. Cells were harvested by removing media, washing with PBS (HyClone, Logan, UT), and then using Accumax cell dissociation enzyme (Innovative Cell Technologies, San Diego, CA) to detach macrophages from the flask followed by the use of a cell scraper.

Isolation and Characterization of EVs from MSCs

MSCs were isolated from human bone marrow from the pelvis of a healthy bone marrow donor (NCT01463475) and identity was confirmed by flow cytometry as previously described [14]. Passage 4 to 8 BM-MSCs were grown in 75-cm^2 flasks to near-complete confluence, washed once with PBS, and placed in StemPro MSC serum-free media (SFM) CTS (A103332-01; Gibco Life Technologies) for 18 to 24 hours. The conditioned culture media (CM) were collected. To prime MSCs to produce LPS exosomes, serum-free media were supplemented with either 100 ng/mL (LPS-low) or 1.0 μg/mL (LPS-high) with *Escherichia coli* LPS O111:B4 (L4391; Sigma, St Louis, MO). EVs were isolated from 4 different BM isolates of MSCs (MSC-EV), LPS-primed MSCs (LPS-low or LPS-high), or macrophages (macrophage-EV) by a 2-step centrifugation process as described [19]. Briefly, the CM was centrifuged using an Allegra X-15R centrifuge (Beckman Coulter, Indianapolis, IN) at $2000 \times g$ at 4°C for 20 minutes. Clarified supernatant was centrifuged in an Optima L-80XP Ultracentrifuge (Beckman Coulter) at $100{,}000 \times g_{avg}$ at 4°C for 2 hours with a SW 28 rotor to pellet exosomes. The supernatant was carefully removed, and EV-containing pellets were resuspended in PBS and pooled. For use and quantitation, we typically suspended the final EV pellet at 100 μL PBS/10 mL CM.

EVs were characterized for protein and RNA concentration using a NanoDrop spectrophotometer (Thermo-Fisher, Waltham, MA). Mean and mode particle diameter and particle concentration were assessed at ZenBio using an IZON qNano Nanoparticle Characterization instrument (ZenBio, Research Triangle Park, NC) and compared using a Nanosight NS300 (Malvern, UK). Residual LPS levels were determined using a chromogenic Limulus amebocyte lysate assay (VRL/Eurofins, Centennial, CO) in EVs of both unstimulated and LPS-stimulated MSCs. To visualize the EVs by transmission electron microscopy, the resuspended EVs were layered on a 30% sucrose cushion and recentrifuged at $100{,}000\ g_{avg}$ at 4°C for 2 hours, and the upper portion of the cushion was collected and recentrifuged. The pellet was resuspended in a small volume of PBS, whole mounted on Formvar EM grids, and stained with uranyl acetate as described [19].

Education of Macrophages by EVs Derived from MSCs or by MSC Coculture

For education of macrophages with exosomes, day 7 macrophages were supplemented with fresh media and treated for 3 days with MSC-EVs, MSC-LPS-low EVs, MSC-LPS-high EVs, or macrophage-EV preparations. Educated macrophages were never directly treated with LPS, but the residual LPS concentration from MSC-LPS-high EV preparations was 1.2 ± 0.65 μg/mL (mean $\pm$ SD), similar to the concentration used during MSC priming. Then, 6 μL of the EV preparation was used to educate 1×10^6 macrophages in 10 mL media. Macrophages not treated with exosomes were designated as "control" macrophages. Macrophages treated after EV treatment were designated as EV/EEMs, LPS-low EEMs, LPS-high EEMs, and macrophage-EEMs, respectively. The amount of the exosome preparation (particles/mL of culture) used for education was standardized between groups.

Cytokine/Chemokine/Growth Factor Multiplex ELISA

Day 10 macrophages (10^6/well) were grown in 6-well plates. The cells were washed with PBS, replaced with culture media, and incubated for 24 hours. The culture media were recovered, centrifuged at 300 x g for 10 minutes to remove any floating cell debris, and assayed for secreted factors using a Milliplex MAP cytokine/chemokine multiplex magnetic bead panel (HCYTOMAG-60K; Millipore, Burlington MA), including epidermal growth factor (EGF); fibroblast growth factor 2 (FGF-2); eotaxin; transforming growth factor β; G-CSF; FMS-like tyrosine kinase 3 ligand (FLT-3L); GM-CSF; chemokine (C-X3-C motif) ligand 1; interferon α2; interferon-γ; growth-related oncogene; C-C motif chemokine 22; platelet-derived growth factor BB (PDGF-BB); soluble CD40 ligand (sCD40L); IL-1ra, IL-1a, IL-1b, IL-2, IL-4, IL-5, IL-6, IL-7, IL-8, IL-9 IL-10, IL-12p40, IL-12p70, IL-13, IL-15, and IL-17; interferon-γ-induced protein 10; monocyte chemoattractant protein 1; monocyte chemoattractant protein 3; macrophage inflammatory protein 1a; macrophage inflammatory protein 1b; regulated on activation, normal T cell expressed and secreted; tumor necrosis factor α; tumor necrosis factor β; and vascular endothelial growth factor A (VEGF-A). Then, 25 μL of culture media was assayed in duplicate as directed by the manufacturer and detected on a Luminex xMAP (Luminex Corporation, Madison, WI) platform.

Phagocytic Assay

Phagocytic assays were performed using the pHrodo Green *E coli* bioparticle conjugate system (cat. P35366; Invitrogen) according to the manufacturer's recommendations. Activation of fluorescence of the pHrodo Green in this system is pH dependent and is detected only when internalized within the phagosome of the cell. Green *E coli* Bioparticle conjugate was reconstituted in PBS, diluted in media, and incubated with the cells for 1 hour at 37°C. Cells were then washed with cold PBS 3 times to reduce nonspecific attachment collected using a cell scraper. Collected macrophages were then treated with Fc Receptor blocker for 10 minutes and stained for 20 minutes at 4°C with PerCP 5.5-CD14 and with APC-CD90 (5E10, cat. 328113; Biolegend, San Diego, CA) for gating of MEMs. CD14-positive/pH pHrodo Green-positive cells at an excitation/emission of 509/533 nm were detected on the MACSQuant analyzer 10 (Miltenyi Biotec) and analyzed using FlowJo software (FlowJo, Ashland, OR).

Acute radiation syndrome in vivo model

Male and female NOD.Cg-*Prkdc*^{scid} *Il2rg*^{tm1Wjl}/SzJ (NSG) mice were purchased from The Jackson Laboratory (Bar Harbor, ME) and used at 8 to 16 weeks of age. All animals were bred and housed in a pathogen-free facility throughout the study. The Animal Care and Use Committee at the University of Wisconsin approved all experimental protocols.

On day 0, age-matched NSG male and female mice received 4 Gy lethal total body irradiation using an X-RAD 320 X-ray irradiator (Precision X-Ray, North Branford, CT). Four hours after radiation injury, mice were treated intravenously in the tail vein with 100 μL PBS or 1×10^6 human MSCs, 1×10^6 control macrophages, 1×10^6 LPS-stimulated macrophages, 1×10^6 EEMs, 1×10^6 LPS-low EEMs, or 1×10^6 LPS-high EEMs. Mice were monitored at least 3 times a week for clinical scores and survival. Clinical scores were determined based on a modified clinical scoring system as previously described [20]. The mice were euthanized if the cumulative clinical score was 6 or greater. For assessing complete blood counts (CBC), mice were bled by nicking the tail vein and collecting blood in a microtainer K_2 EDTA tube (cat. 365974; Becton Dickinson, Franklin Lakes, NJ). Mice were bled before radiation challenge to get baseline values (control) and then postradiation on day 4. Surviving LPS-EEM-treated mice were also collected on day 32 and days 50 to 53. Whole blood was assayed on a Hemavet 950FS analyzer (Drew Scientific, Miami Lakes, FL), and mean values were determined for erythrocytes, leukocytes, and thrombocytes.

Diagnostic necropsy and histologic preparation

Gross necropsy of organ systems consisted of determining both organ weight and organ weight as a function of percent body weight (%BW), as well as the external examination of the integument, cardiovascular, respiratory, digestive, lymphohematopoietic, urogenital, endocrine, central nervous, and musculoskeletal systems. Gross necropsy was performed on the following groups: unirradiated NSG mice and NSG mice postradiation challenge on day 9 (PBS treated and LPS-high EEM treated), day 31 (LPS-high EEM treated), and day 53 (moribund LPS-high EEM treated).

Histology focused on the preparations of slides from sections of spleen and bone marrow from long bones (femur, tibia, humerus), sternum, and pelvis (ilium). Tissues were fixed in 10% neutral buffered formalin and processed on a Sakura (Torrance, CA) Tissue-Tek VIP 6 processor and embedded on a Sakura Tissue-Tek TEC embedding station. Slides were cut on a Leitz (GMI, Ramsey, MN) 2235 microtome at 5 to 6 microns and stained with hematoxylin and eosin using a Sakura Tissue-Tek DRS automatic stainer and manually coverslipped. Tissues were visualized using a Nikon (Melville, NY) Eclipse 50 I microscope at multiple magnifications using the following Nikon objectives: 4×/0.2 Plan Apo, 10× /0.45 Plan Apo, 20× /0.75 Plan Apo, and 40× /0.95 Plan Apo. Photographs were taken using a SPOT model 10.2 camera aided with SPOT acquisition software for MAC 5.2. (SPOT Imaging, Sterling Heights, MI) The BM cellularity was scored by a blinded pathologist using a semiquantitative scale: no loss = 0, minimal loss = 1, mild loss = 2, moderate loss = 3, marked loss = 4, and severe loss = 5.

Statistical analysis

Statistics were performed using GraphPad Prism version 7.0 (GraphPad Software, San Diego, CA). Data were reported as mean ± SEM. Groups of 3 or more were compared using an ordinary 1-way analysis of variance or Kruskal-Wallis test with the Dunn multiple-comparisons post-test. Mantel-Cox log-rank test was used for the comparison of the Kaplan-Meier survival curves. A *P*value less than .05 was considered statistically significant for all tests.

RESULTS

EVs from MSCs Consist Primarily of Exosomes

Transmission electron microscopy images indicated MSC-EVs had the typical appearance of exosomes: a circular shape with a convex center, and the majority (>90%) of EV preparations consisted of exosome-sized vesicles (<200 nm) (Figure 1A). Quantifying EVs of MSCs or macrophages using either a resistive pulse sensing instrument (Figure 1B) or a visual nanoparticle tracking analysis (Figure 1C) indicated that the EVs generally ranged in size from 50 to 185 nm. On the basis of this analysis, we designated EVs as exosomes. The qNano instrument analysis of multiple preparations from different MSC isolates yielded similar profiles in terms of mean particle sizes (mean particle size of 128 nm and mode particle size of 91 nm) and particle density (Supplementary Table S1). Exosomes from LPS-primed MSCs were similar to exosomes from unprimed MSC-exosomes in terms of size (mean particle size of 168 nm and mode particle size of 109 nm) with mean particle concentrations: 1.4×10^{11} particles/mL versus

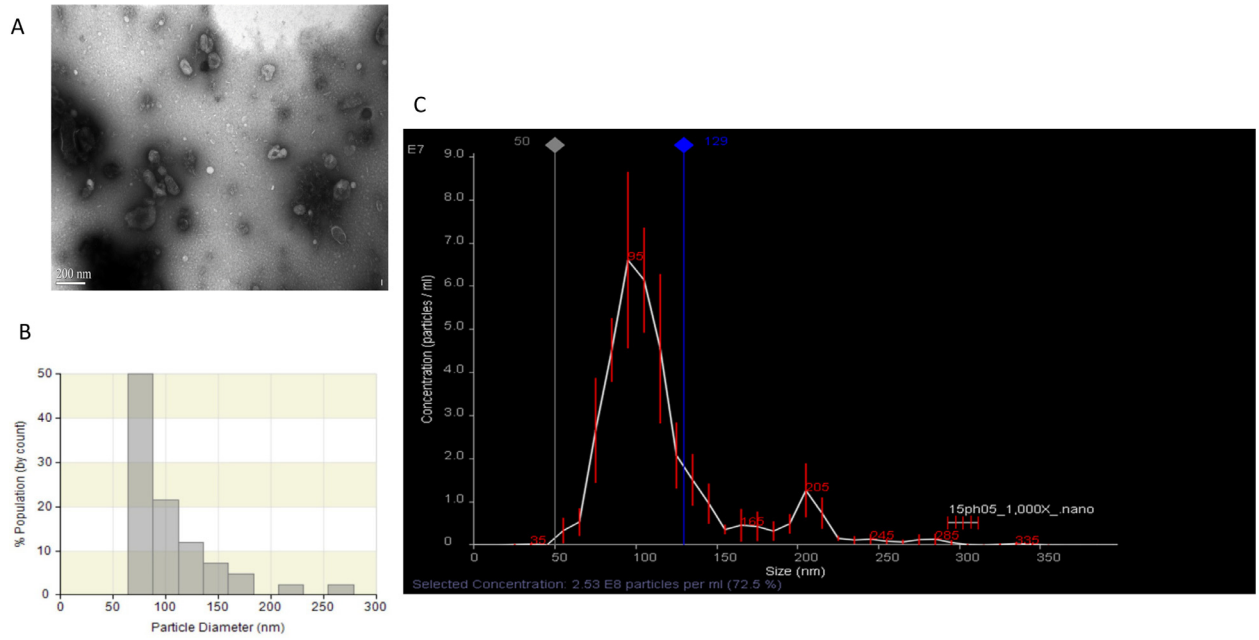

Figure 1. EVs isolated from human MSCs consist primarily of exosome-sized vesicles. EVs were isolated from BM-MSCs, and EVs were analyzed by transmission electron microscopy (TEM) and 2 different instruments to quantify the mean particle diameter. (A) Representative TEM of the EV preparations indicated that the particles had the typical cup-shaped vesicular appearance of EVs and the size was generally less than 200 nm. (B) The preparations characterized by resistive pulse sensing using the qNano Nanoparticle instrument indicated that most of the particles were within the 60- to 130-nm range. (C) The preparations characterized by dynamic light scattering using the Nanosight NS300 indicated that the size of the majority of particles was 95 nm with a range of 50 to 129 nm and generally matched the same profile as the qNano Nanoparticle instrument. Based on these characterizations, the majority of the particles consisted primarily of exosome-sized EVs.

1.1×10^{11} particles/mL for the exosomes from unprimed and LPS-primed MSCs, respectively. LPS levels in EVs from both unstimulated and LPS-stimulated MSCs were 0.008 ± 0.006 μg/mL and 1.2 ± 0.65 μg/mL, respectively. Macrophages were also found to primarily produce exosome-sized particles, with yields about 5-fold more based on cell number (10^6).

EEMs Express a Combination of Classical M2 and M1 Markers Dependent on LPS-Stimulation of MSCs

Next, we used exosomes from unprimed MSCs, MSCs primed with a low dose of LPS, and MSCs primed with a high dose of LPS to generate exosome-educated macrophages (EEMs, LPS-low EEMs, and LPS-high EEMs) and compared their phenotypes by examining cell surface marker expression of M2 markers (CD163, CD206, PD-L1, and PD-L2), M1 markers (CD86 and HLA-DR), and functional markers (CD16, CD39, and CD73). Compared with controls, EEMs expressed significantly higher mean fluorescent intensities for CD206 ($P \leq .0001$), PD-L1 ($P \leq .0001$), and PD-L2 ($P \leq .001$) (Figure 2). LPS-low EEMs also showed elevated expression of CD206, PD-L1, and PD-L2 but also higher CD16 (Figure 2). In contrast, LPS-high EEMs showed no difference in M2 marker expression compared with controls. The M1 markers CD86 and HLA-DR were significantly lower in LPS-low EEMs compared with either controls or EEMs (Figure 2). Although M2 marker expression levels between the LPS-low and LPS-high were different, expression of M1 markers in LPS-high EEMs was actually decreased compared with controls or EEMs. There was a significant increase in the percentage of $CD73^+$ cells for both LPS-low and LPS-high EEMs compared with either controls or EEMs (Supplementary Figure S1). Thus, LPS-high EEMs do not show increased expression of M1 or M2 markers but do have an increased percentage of CD73.

LPS-High EEMs Protect Mice from Lethal Radiation Injury and Promote Hematologic Recovery

To determine if exosomes from MSCs could generate macrophages that mediate radioprotection, EEMs, LPS-low EEMs, and LPS-high EEMs were infused as a single treatment to NSG mice after a lethal dosage of radiation. Recipients of LPS-high EEMs showed improved survival ($P \leq .0001$, Figure 3A), whereas cell treatments with MSCs, macrophages, or EEMs at the same dose were ineffective. Only LPS-high EEMs treatment led to a significant reversal of ARS and prolonged survival, with a median survival of 47.5 days, compared with 8 to 14 days in the other groups. Although there was an initial delay in recovery of weight and clinical score in the LPS-high EEM-treated mice, by day 10, the mean percent weight change ($P < .05$, Figure 3B) and mean clinical score ($P < .05$, Figure 3C) steadily began to improve and remained at near-normal levels for several weeks. About 70% of the LPS-high EEM-treated mice were alive at this point, whereas 20% of the mice treated with LPS-low EEMs survived long term, indicating that potency of the exosomes appears to be related to concentration of LPS used to stimulate the MSCs. Overall, the protective effect from LPS-high EEM treatment lasted until day 38 (Figure 3C); thereafter, the cumulative clinical scores progressively worsened and the remaining mice died between days 50 and 53.

LPS-high EEM treatment was also found to significantly restore CBCs in mice after lethal ARS (Table 1). At day 4, all irradiated mice showed signs of radiation injury and developed general pancytopenia. Interestingly, the greatest significant drop in leukocyte cell subsets (neutrophils, lymphocytes, and monocytes) was detected in LPS-high EEM-treated mice. Moreover, there was a significant reduction in platelets (Table 1, day 4). Overall, we were unable to identify a candidate cell subtype that could be a predictable biomarker for survival in LPS-high EEM-treated mice. By day 20, the only remaining group available for further CBC analysis were recovering LPS-high EEM-treated mice. During this recovery period, as assessed by weight and clinical scores, these mice were rebled at day 32. Leukocyte subsets were all restored to normal levels and platelets improved, although not quite to normal levels (Table 1, day 32). However, platelet volume was significantly greater, suggesting more immature platelets in the

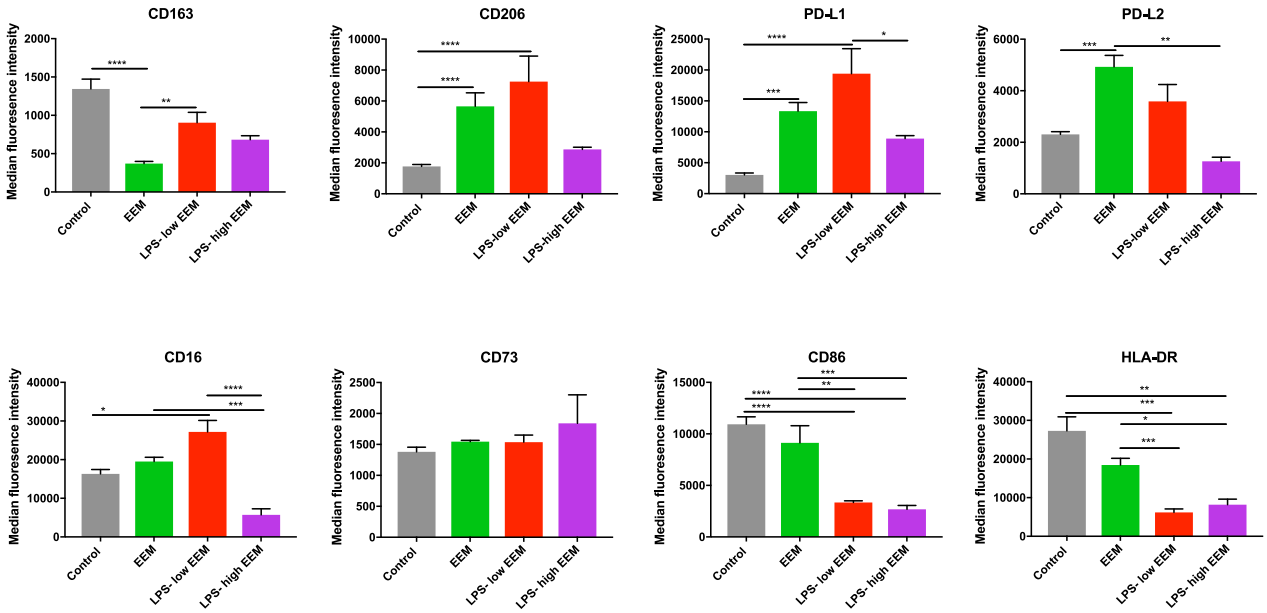

Figure 2. Human LPS-high EEMs express low levels of M1 markers CD16, CD86, and HLA-DR. Day 7 macrophages were either untreated (Control) or treated with exosomes from MSCs to produce EEMs, LPS-low EEMs, or LPS-high EEMs. The median fluorescence intensity (MFI) of $CD14^+$cells for each marker (± SEM) is shown. Results pooled from 2 separate experiments, with 4 to 13 samples/group. Groups compared by Kruskal-Wallis with a Dunn post-test. $^*P \leq .05$, $^{**}P \leq .005$, $^{***}P \leq .0005$, $^{****}P \leq .0001$ between groups is designated by bars.

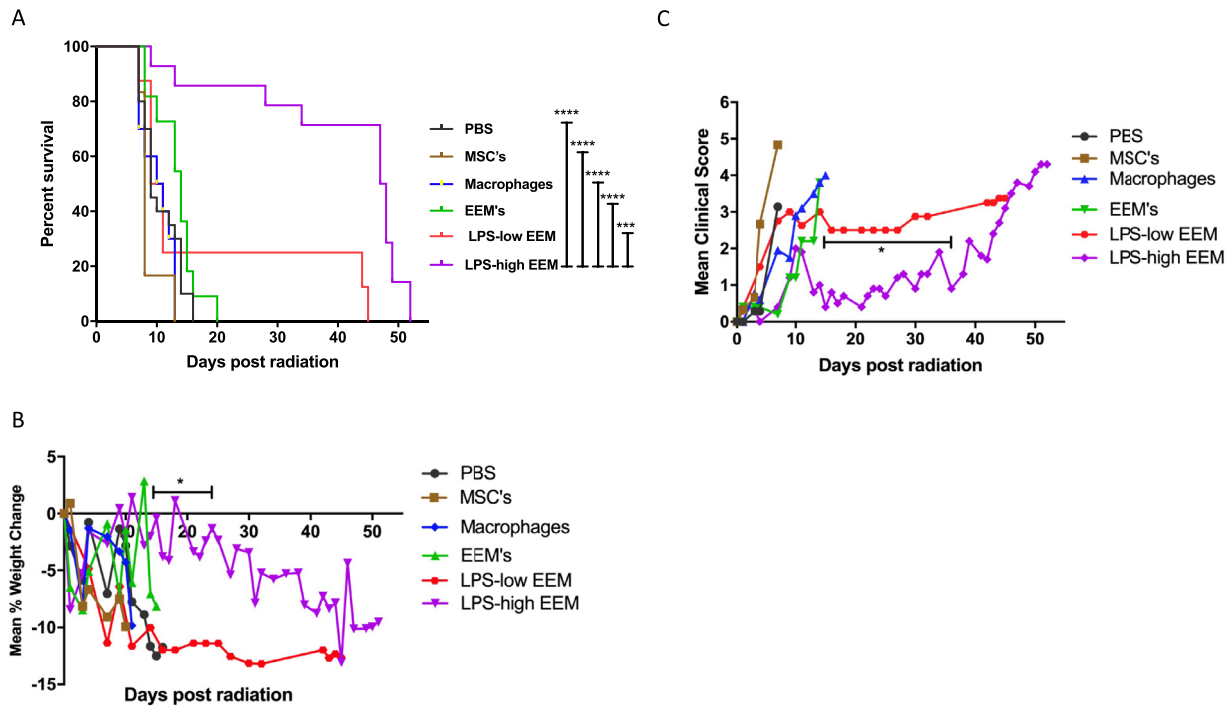

Figure 3. Treatment with human LPS-high EEMs significantly improves survival, weight loss, and clinical scores in mice after lethal radiation injury. (A-C) On day 0, NSG mice received 4 Gy of lethal radiation followed by an i.v. treatment 4 hours later with PBS (vehicle control), 1×10^6 MSCs, 1×10^6 macrophages, 1×10^6 EEMs, 1×10^6 LPS-low EEMs, or 1×10^6 LPS-high EEMs. (A) Survival curve of treated mice after radiation. (B) Mean percent weight change compared with PBS controls. (C) Mean clinical scores (percent weight loss, posture, activity, and fur texture) compared with MSC and/or PBS controls. The final mean percent weight change and clinical score were carried over after death to allow for comparison by Kruskal-Wallis with a Dunn post-test between groups at a given time point. Results pooled from 2 separate experiments, with 7 to 21 mice/group. $^*P < .05$, $^{***}P \leq .005$, $^{****}P \leq .0001$.

periphery. At days 50 to 53, when the mice became moribund, there was a slight drop in platelets, but the other blood cell subsets did not drop significantly (Table 1, days 50 to 53). Thus, a single treatment with LPS-high EEMs was able to support normal hematopoiesis, even during later clinical deterioration, indicating the terminal diagnosis during clinical symptom relapse was not due to a failure in hematopoiesis. Histopathologic examination of major organs from day 50 to 53 moribund mice indicated that the probable terminal diagnosis was hepatic hypoxic necrosis (with a predominantly centrilobular pattern), a skin infection, or a combination of both (Supplementary Figure S3). No cultures or other testing were performed to identify the causative organism, but skin features were suspicious for *Corynebacterium bovis*.

To determine the contribution of residual LPS in the exosome preparations isolated after MSC priming on direct macrophage stimulation, we compared treatment of LPS-stimulated macrophages to no treatment (PBS), unstimulated macrophages, and LPS-high EEM treatment of lethally irradiated mice. We found that LPS-stimulated macrophages resulted in 100% lethality akin to mice receiving no treatment or unstimulated macrophages. Only recipients of LPS-high EEMs showed significantly improved survival (Supplementary Figure S4).

LPS-High EEM Treatment Protected Hematopoietic Tissue in Bone Marrow and Spleen from Radiation Injury

To identify which organs and tissues may be protected by LPS-high EEM treatment, we compared histology of BM from long bones (Figure 4A) and spleens (Figure 4B) of normal nonirradiated mice to irradiated mice with or without treatment at different times postchallenge. By gross necropsy, the spleens were most affected by a 4-Gy radiation exposure, whereas overt changes to the heart, liver, and kidneys were less obvious (data not shown). Spleens from irradiated moribund PBS-treated

Table 1
Impact of Human LPS-High EEM Treatment on Complete Blood Counts after Lethal Irradiation

Group	Day Postradiation	RBC (M/μL)	WBC (K/μL)	Neutrophils (K/μL)	Lymphocytes (K/μL)	Monocytes (K/μL)	Platelets (K/μL)	Platelet Volume (fL)
Control	NA	4.6	1.37	1.06	0.21	0.065	608	4.5
PBS	4	4.3	0.49*	0.14†	0.24	0.03	191†	4.3
EEM	4	3.7	0.19†	0.03†	0.08	0.013	219†	4.2*
LPS-high EEM	4	3.7*	0.21‡	0.02‡	0.05*	0.01†	187‡	4.5
LPS-high EEM	32	4.1	1.68	1.21	0.36	0.05	379*	5.0‡
LPS-high EEM	50-53	5.8	1.48	0.92	0.4	0.11	316†	5.0‡

NA indicates Not applicable.
* $P \leq .05$.
† $P \leq .005$.
‡ $P \leq .0005$.

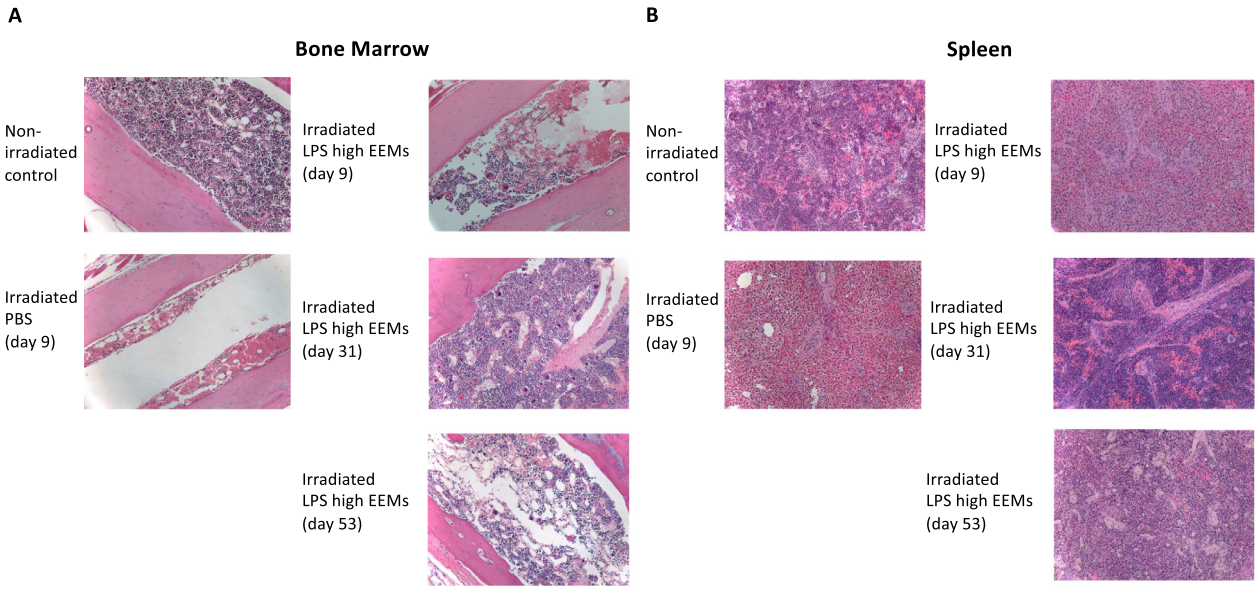

Figure 4. Human LPS-high EEM treatment protects against tissue damage in the BM and spleen of mice after lethal radiation injury. On day 0, NSG mice received either no radiation (normal healthy) or 4 Gy of lethal radiation followed by an i.v. treatment 4 hours later with PBS or with 10^6 cells of LPS-high EEMs. Histology on tissue preparations of BM from femurs and spleens of healthy mice was compared to day 9 postradiation PBS controls and LPS-high EEMs, day 31 LPS-high EEMs, or day 53 LPS-high EEMs. (A) Representative 20× images of hematoxylin and eosin (H&E)-stained femoral BM sections from each group. (B) Representative 20× images of H&E-stained spleen sections.

mice were significantly smaller in mean weight and percent spleen BW (9.3 mg and 0.05%) compared with healthy controls (28.1 mg and 0.11%) ($P < .05$). In contrast to the irradiated PBS-treated mice, mean spleen weight and percent spleen BW from LPS-high EEM-treated mice during both the recovery phase at day 31 (34.4 mg/0.15%) or even during clinical symptom relapse at days 50 to 53 (25.1 mg/0.13%) were both similar to healthy controls. Compared to the histologic sections of BMs and spleens from healthy mice (Figure 4A,B), moribund PBS-treated mice at day 9 postirradiation showed a marked absence of hematopoietic cellularity in the BM and total lack of extramedullary hematopoiesis in the spleen with clear hemorrhage (Figure 4A,B). In contrast, there were markedly more hematopoietic cells present in the LPS-EEM-treated mice at day 9 postirradiation (Figure 4A,B). At this time, cumulative cellularity present in the BM cavity (long bones, sternum, and pelvis) graded from 0 to 5 (indicating most to least degree of cellularity) was significantly better in LPS-high EEM mice compared with untreated mice ($P < .01$) (Table 2). Improvement continued in these mice at day 30 with strong to moderate hematopoietic activity in the BM of the long bones but also in the pelvis and sternum. The cumulative cellularity improved to near-normal levels in LPS-EEM-treated mice at scores of 0.5 ± 0.5 (Table 2), with an intense hematopoietic component present in the spleen (Figure 4A,B). Interestingly, even during clinical symptom relapse at day 53, hematopoietic tissue in the BM and spleen was still distinctly present (Figure 4A,B) in the LPS-high EEM-treated mice, similar to what we observed in CBCs. Cellularity in the long bones, sternum, and pelvis in these mice was high at 1.4 ± 0.8.

LPS-EEMs Have a Distinct Gene Expression and Cytokine Profile

To examine potential mechanisms of protection against ARS and promotion of hematopoietic recovery, we next examined the gene expression profile of the macrophage subsets by quantitative PCR. Both LPS-low and LPS-high EEMs showed a similar profile with significant increases in *VEGF-A* (LPS-low $P = .018$ and LPS-high $P = .006$) and *STAT1* (LPS-low $P = .022$ and LPS-high $P = .033$) compared with control macrophages (Supplementary Figure S2). However, there were differences between LPS-low and LPS-high EEMs; LPS-high EEM only showed increased expression of *STAT3* ($P = .048$) compared with control macrophages (Supplementary Figure S2).

To verify changes in gene expression at the protein level, we also quantified production of cytokines and growth factors by each macrophage subset. LPS-low EEMs and LPS-high EEMs secreted significantly higher level(s) of factors involved in

Table 2
Bone Marrow Cellularity

Group	Day Postradiation Challenge	Long Bones (Femur, Tibia, Humerus)	Sternum	Pelvis	Cumulative
Healthy controls	NA	0.0 ± 0.0	0.0 ± 0.0	0.0 ± 0.0	0.0 ± 0.0
Untreated controls	9	4.6 ± 0.4	4.3 ± 0.7	4.3 ± 0.4	4.3 ± 0.7
LPS-high EEMs	9-10	4.0 ± 1.0	3.3 ± 0.7	4.1 ± 0.2	3.8 ± 0.6**
LPS-high EEMs	31	1.0 ± 0.9	0.25 ± 0.7	0.3 ± 0.1	0.5 ± 0.7****
LPS-high EEMs	50-53	1.9 ± 0.4	0.9 ± 0.7	1.5 ± 1.3	1.4 ± 0.8****

Key: No loss = 0; minimal loss = 1; mild loss = 2; moderate loss = 3; marked loss = 4; severe loss = 5.
** $P < .05$.
**** $P < 0.0001$

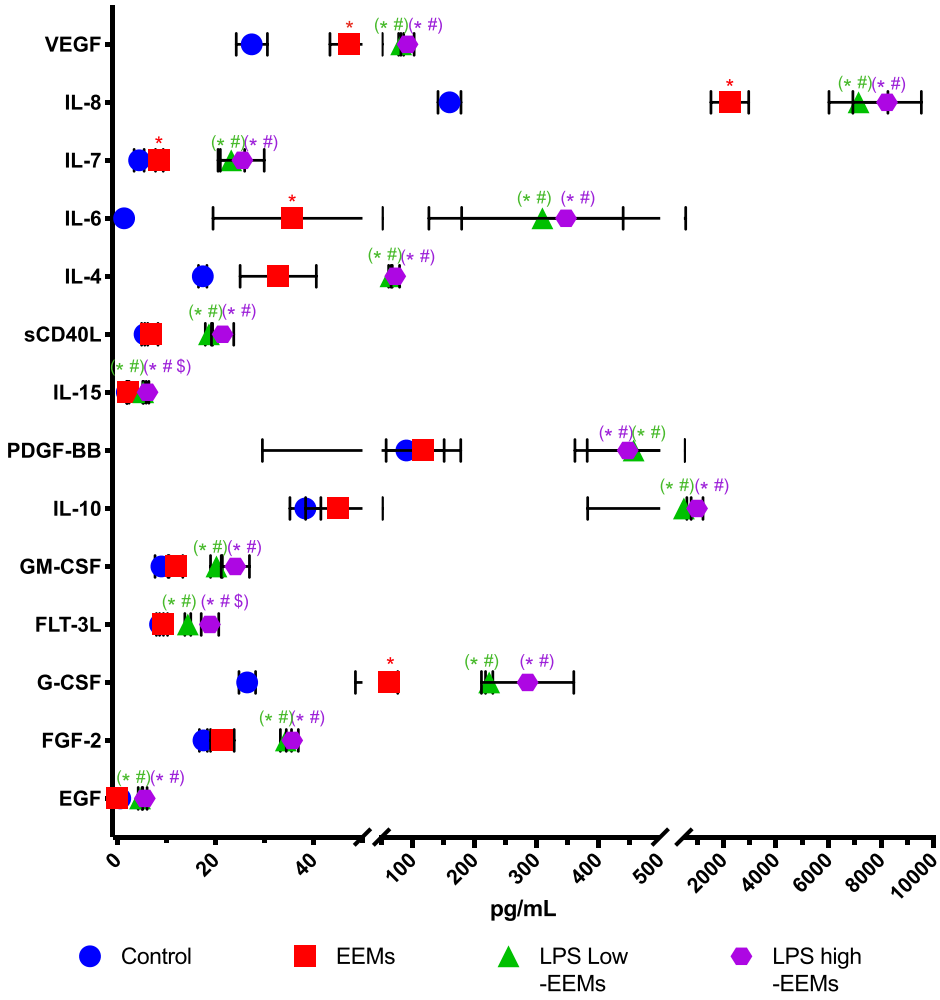

Figure 5. Human LPS-high EEMs secrete high levels of anti-inflammatory cytokines and growth factors by multiplex ELISA. Day 7 macrophages were either untreated (control) or treated with exosomes from MSCs for 3 days to produce EEMs and LPS-low or LPS-high EEMs. Cells were then washed and supernatants collected after 24 hours and assayed. Samples were run in triplicate and compared to control (*), EEMs (#) or LPS-low EEMs ($) and compared by ANOVO with a Dunn post test $^{*}P \leq .05$, $^{**}P \leq .01$, $^{***}P \leq .001$, $^{****}P \leq .0001$.

tissue repair compared with control macrophages, including cytokines (IL-4 [$P < .001$], IL-8 [$P < .01$]), growth factors (EGF [$P < .001$], FGF-2 [$P < .001$], VEGF-A [$P < .001$]), T and natural killer cell growth factors (IL-7 [$P < .01$], IL-15 [$P < .0001$]), platelet growth and activation factors (sCD40L [$P < .001$], PDGF-BB [$P < .05$]), and hematopoietic growth factors (FLT-3L [$P < .05$], G-CSF [$P < .05$], and GM-CSF [$P < .01$]) (Figure 5). Moreover, many of these secreted factors were also significantly higher than that found for EEMs. Although the types of factors secreted by either the LPS-low or LPS-high EEMs were very similar, the concentrations secreted by LPS-high EEMs were greater than LPS-low EEMs. Interestingly, IL-10 ($P = .05$), FLT-3L ($P < .05$), and IL-15 ($P < .05$) were found to be significantly higher in LPS-high EEMs (Figure 5).

LPS-High EEMs Show Increased Phagocytic Activity

Active phagocytic function in macrophages is important for both wound healing and tissue remodeling [21]. Phagocytic activity, as measured by the percentage of cells containing internalized pHrodo Green *E coli* particles (percent cells), was found to be highest in LPS-high EEMs (Figure 6). Phagocytic activity between the controls and EEMs was not significantly different. However, LPS-low EEMs ($P \leq .0001$) and LPS-high EEMs ($P \leq .0001$) were significantly more phagocytic than controls. In contrast, M1 macrophages were significantly less phagocytic (42%) compared with controls (59%, $P \leq .0005$). Thus, the macrophage subsets that are effective in this ARS model seem to have increased phagocytic activity, perhaps indicating a functional biomarker and role for tissue remodeling.

DISCUSSION

The goal of this study was to develop a cell-based therapy that would be effective at preventing or treating ARS. Macrophages are an important cell subset involved in wound healing and tissue remodeling. At the site of injured tissue, macrophages can clear the site of pathogens or cell debris, regulate inflammation, and promote tissue repair [22,23]. Previously we have shown that macrophages educated after coculture with MSCs were more effective than MSCs alone in treating ARS in vivo in part by promoting fibroblast proliferation [15]. However, a coculture methodology can be challenging to translate to the clinic, because one would have to eliminate MSCs from the macrophage culture before infusion or infuse 2 different types of cells simultaneously. Herein we show that exosomes isolated from MSCs can replace cocultivation and, when derived from MSCs primed with LPS, can educate

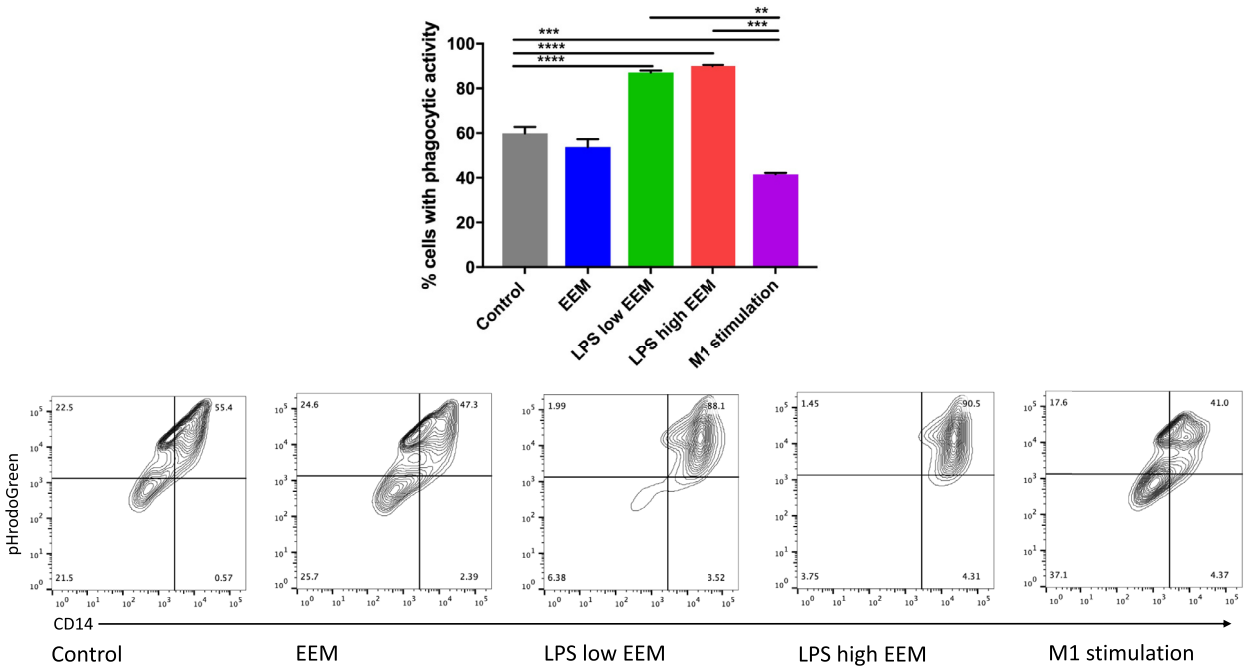

Figure 6. LPS-high EEMs are strongly phagocytic using pHrodo Green *Escherichia coli* bioparticles. Day 7 macrophages were either untreated (control) or treated for 3 days using exosomes from MSCs to produce EEMs and LPS-low or LPS-high EEMs or stimulated with M1 factors (Phorbol 12-myristate 13-acetate/IFN-γ/LPS) to produce M1-stimulated macrophages. Day 10 macrophages were treated with pHrodo Green *E coli* bioparticles and the ratio of $CD14^+$ cells positive for phrodo Green *E coli* bioparticles (designated as percent cells) was determined by flow cytometry. Samples were pooled from 2 separate experiments and compared by analysis of variance with a Dunn post-test, 3 to 5 samples/group. $^*P \leq .05$, $^{**}P \leq .005$, $^{***}P \leq .0005$, $^{****}P \leq .0001$ between groups is designated by bars.

macrophages to mediate protection from ARS in vivo, in part by preserving host hematopoiesis.

MSC-EVs are produced in large numbers and consist of both large (1000 nM) microvesicles and smaller (100 nM) exosomes known to contain micro-RNA, proteins, and DNA that can influence the gene expression and functionality of recipient cells [24-27]. MSC-EVs can influence tissue responses to injury, infection, and disease, and their function appears to reciprocate the direct use of MSCs [24,28]. Indeed, there is a great deal of interest in the therapeutic potential of EVs alone for the treatment of various diseases and tissue repair [29]. Numerous animal studies have indicated that MSC-EV treatments are effective as a sole therapy in brain, heart, liver, and kidney injury models [24]. For ARS treatment, MSC-EVs have been shown to rescue murine marrow hematopoietic cells after sublethal radiation [30]. Moreover, the contents of MSC-EVs are not static and can be altered by MSC exposure to different stimuli. A recent study indicated that MSCs primed with bacterial LPS, a Toll-like receptor 4 ligand, produced MSC-EVs that were better at promoting wound healing in diabetic rats and thought to be due to the polarization of endogenous macrophages in the tissue [31]. Our analysis of multiple human isolates indicated that MSCs reproducibly produced exosomes of similar size and quantity. Unlike a previous report [31], we did not detect any significant increase in exosome concentration after priming of MSCs at either low or high dosages of LPS (Supplementary Table S1). Overall, this consistency in exosome secretion provides an attractive translatable option for commercial production by MSCs.

Current dogma indicates that stimulation of MSCs with proinflammatory signals like LPS should promote a proinflammatory phenotype. Indeed, direct injections of LPS are being studied in clinical trials as an adjuvant to stimulate inflammation and boost innate immunity [32]. Therefore, one might expect that macrophages treated with exosomes from MSCs stimulated with LPS would generate a M1 macrophage that would be not only ineffective but also more destructive in an ARS model. However, when macrophages were educated with exosomes from LPS-primed MSCs, we observed a reparative phenotype that extended survival, repaired tissue damage in the spleen and bone marrow, and promoted hematopoiesis. This outcome was dependent on LPS and its concentration, as exosomes from MSCs primed with a high concentration of LPS (LPS-high EEMs) improved weight loss, showed lower clinical scores, and extended overall survival in an ARS model, with quantifiable improvements by CBC and repairing of hematopoietic tissue in the BM and spleen. Notably, there was initially a decrease in "leaky-SCID" lymphocytes observed in vivo, which may have decreased the overall inflammatory response to radiation, leading to a significant restoration in the leukocyte cell panel, along with significant increases in platelet volume—all indications of the resumption of hematopoietic activity. Studies have indicated the importance of macrophages in supporting and maintaining hematopoietic stem cells [33-35]. We hypothesize that because the MSCs are strong homeostatic regulators, exposure to strong inflammatory environmental ques, such as high LPS levels, compels them to direct effector cells like macrophages to respond in a counterbalancing way and become more anti-inflammatory.

To examine this hypothesis, we characterized the macrophage subsets by cell surface marker expression, gene expression, cytokine/growth factor secretion, and phagocytic activity. Distinctly in LPS-high EEMs, increased gene expression of *STAT3* was noted compared with control macrophages. Increased protein expression of IL-10 (an important anti-inflammatory cytokine), VEGF-A (a growth factor involved in

angiogenesis), and IL-8 (a cytokine involved in stimulating phagocytosis) was also observed [36]. By flow cytometry, the LPS-high EEMs displayed a unique surface profile, expressing very low levels of M1 markers (CD86 and HLA-DRs) and the proinflammatory marker, CD16 [37]. Another relevant surface marker was CD73, expressed in significantly higher percentages of LPS-high EEMs. CD73 is an ectonucleotidase that converts Adenosine monophosphate to adenosine and thought to be both immunosuppressive and angiogenic [15,38], each important in wound repair. Because MEMs were previously described to be effective in treating ARS in vivo [15], the shared phenotype of LPS-high EEMs and MEMs (low expression of M1 markers with high expression of CD73) may be an important "release criterion" that could be used to designate successful education by MSCs. Nevertheless, it should be noted that although characteristics found in LPS-high EEMs were significantly different from controls, often there were no differences between LPS-low and LPS-high EEMs, indicating some biologic features are a result of education with LPS-stimulated MSCs independent of LPS dose.

LPS-high EEMs were found to secrete significantly greater amounts of cytokines and growth factors compared with the other treatment groups. These factors likely helped to re-establish normal blood counts in the mice and possibly were involved in the restoration of clinical scores in the mice with ARS. Factors important for tissue remodeling such as EGF, FGF-2, PDGF-BB, sCD40L, and VEGF-A were elevated in LPS-high EEMs. Moreover, there were increases in growth factors such as IL-7 and G-CSF, which function to restore T cells and neutrophils, respectively. As seen by gene expression and flow cytometry, the overall secretory profile of LPS-high EEMs was very similar to LPS-low EEMs; two growth activating factors (FLT-3L, a stem cell growth factor that stimulates the growth of blood progenitors, and IL-15, which regulates the activation and proliferation of T cells and natural killer cells) were significantly higher in LPS-high EEMs. These 2 factors may be the major drivers of hematopoietic recovery and could be blocked in preclinical models to see if the radioprotective effects are abrogated.

Recent studies suggest a strong link between phagocytic macrophages and tissue repair; deficits in macrophage phagocytic function can lead to the pathogenesis of nonhealing wounds often seen in diabetes or during aging [21]. The LPS-high EEMs were found to possess the highest percentage of phagocytic cells compared with all the other groups. An important function of wound macrophages is the ability to remove neutrophils after the decontamination phase of wound healing, and evidence indicates that neutrophils negatively influence repair in part because they are capable of destroying normal tissue [21]. Besides actively ingesting neutrophils, phagocytic macrophages can also induce apoptosis, which prevents secondary necrosis, and is thought to be essential for complete repair [21]. Besides the LPS-high EEMs, the LPS-low EEMs and MEMs shown previously also had significantly higher phagocytic ability and interestingly were the only groups to show any efficacy in the ARS model [15]. These results indicate the importance of phagocytic capacity for the treatment of radiation damage from ARS.

In summary, we show that exosomes from MSCs stimulated by LPS can educate macrophages into a radioprotective phenotype capable of affecting cytokine secretion and increasing phagocytic activity in vitro and promoting hematopoiesis and tissue repair in vivo. These effects were associated with improved survival from ARS in vivo. To move these findings toward an "off-the-shelf" cell therapy for ARS, we envision the use of frozen allogeneic macrophages that were pre-educated with exosomes from LPS-stimulated MSCs. Because residual LPS is present in exosome preparations isolated after MSC priming, some of the changes in macrophage phenotype by flow cytometry, gene expression, and cytokine/growth factor secretion may be confounded by LPS alone or in conjunction with the contents of the exosomes. This caveat should be considered when characterizing any cells generated from LPS-primed MSC-EVs. Future studies should focus on establishing biomarkers that predict successful generation of radioprotective cells ex vivo and cell subsets in vivo that contribute to improved hematopoiesis and in better understanding the mechanisms used by LPS-high EEMs to protect against lethal ARS.

DECLARATION OF COMPETING INTEREST

P.H. and C.M.C. have a patent related to this publication (US Patent 10,166,254 B2). The authors declare that no other relevant financial conflicts of interest exist.

ACKNOWLEDGMENTS

Financial disclosure: This study was supported by the University of Wisconsin Carbone Cancer Center (UWCCC) Flow Cytometry and Experimental Pathology (National Institutes of Health [NIH]/National Cancer Institute [NCI] P30 CA014520) and in part by the Don Anderson GVHD Fund and Crystal Carney Fund for Leukemia Research (P.H.), St. Baldrick's-Stand Up To Cancer Pediatric Dream Team Translational Research Grant SU2C-AACR-DT-27-17, NIH/National Center for Advancing Translational Sciences UL1TR000427 to the University of Wisconsin Institute for Clinical and Translational Research and NIH/NCI P30 CA014520 to the UWCCC (P.H. and C.M.C.), and NIH/NCI K08 CA174750 (C.M.C). Stand Up To Cancer is a division of the Entertainment Industry Foundation. Research grants are administered by the American Association for Cancer Research, the scientific partner of SU2C. The contents of this article do not necessarily reflect the views or policies of the Department of Health and Human Services, nor does mention of trade names, commercial products, or organizations imply endorsement by the US government. None of these funding sources had any input in the study design, analysis, manuscript preparation, or decision to submit for publication.

SUPPLEMENTARY MATERIALS

Supplementary data related to this article can be found online at doi:10.1016/j.bbmt.2019.07.026.

REFERENCES

1. Williams JP, Brown SL, Georges GE, et al. Animal models for medical countermeasures to radiation exposure. *Radiat Res*. 2010;173(4):557–578.
2. Fliedner TM, Chao NJ, Bader JL, et al. Stem cells, multiorgan failure in radiation emergency medical preparedness: a U.S./European Consultation Workshop. *Stem Cells*. 2009;27(5):1205–1211.
3. Singh VK, Seed TM. A review of radiation countermeasures focusing on injury-specific medicinals and regulatory approval status, part I: radiation sub-syndromes, animal models and FDA-approved countermeasures. *Int J Radiat Biol*. 2017;93(9):851–869.
4. Singh VK, Garcia M, Seed TM. A review of radiation countermeasures focusing on injury-specific medicinals and regulatory approval status, part II: countermeasures for limited indications, internalized radionuclides, emesis, late effects, and agents demonstrating efficacy in large animals with or without FDA IND status. *Int J Radiat Biol*. 2017;93(9):870–884.
5. Singh VK, Newman VL, Seed TM. Colony-stimulating factors for the treatment of the hematopoietic component of the acute radiation syndrome (H-ARS): a review. *Cytokine*. 2015;71(1):22–37.
6. Koc ON, Gerson SL, Cooper BW, et al. Rapid hematopoietic recovery after coinfusion of autologous-blood stem cells and culture-expanded marrow mesenchymal stem cells in advanced breast cancer patients receiving high-dose chemotherapy. *J Clin Oncol*. 2000;18(2):307–316.
7. Pittenger MF, Mackay AM, Beck SC, et al. Multilineage potential of adult human mesenchymal stem cells. *Science*. 1999;284(5411):143–147.

8. Bernardo ME, Fibbe WE. Mesenchymal stromal cells: sensors and switchers of inflammation. *Cell Stem Cell*. 2013;13(4):392–402.
9. Eaton Jr EB, Varney TR. Mesenchymal stem cell therapy for acute radiation syndrome: innovative medical approaches in military medicine. *Mil Med Res*. 2015;2:2.
10. Hu KX, Sun QY, Guo M, Ai HS. The radiation protection and therapy effects of mesenchymal stem cells in mice with acute radiation injury. *Br J Radiol*. 2010;83(985):52–58.
11. Lange C, Brunswig-Spickenheier B, Cappallo-Obermann H, et al. Radiation rescue: mesenchymal stromal cells protect from lethal irradiation. *PLoS One*. 2011;6(1):e14486.
12. Shim S, Lee SB, Lee JG, et al. Mitigating effects of hUCB-MSCs on the hematopoietic syndrome resulting from total body irradiation. *Exp Hematol*. 2013;41(4):346–353.
13. Hu J, Yang Z, Wang J, et al. Infusion of Trx-1-overexpressing hucMSC prolongs the survival of acutely irradiated NOD/SCID mice by decreasing excessive inflammatory injury. *PLoS One*. 2013;8(11):e78227.
14. Kim J, Hematti P. Mesenchymal stem cell-educated macrophages: a novel type of alternatively activated macrophages. *Exp Hematol*. 2009;37(12):1445–1453.
15. Bouchlaka MN, Moffitt AB, Kim J, et al. Human mesenchymal stem cell-educated macrophages are a distinct high IL-6-producing subset that confer protection in graft-versus-host-disease and radiation injury models. *Biol Blood Marrow Transplant*. 2017;23(6):897–905.
16. Caplan AI, Correa D. The MSC: an injury drugstore. *Cell Stem Cell*. 2011;9(1):11–15.
17. Pittenger M. Sleuthing the source of regeneration by MSCs. *Cell Stem Cell*. 2009;5(1):8–10.
18. Waterman RS, Tomchuck SL, Henkle SL, Betancourt AM. A new mesenchymal stem cell (MSC) paradigm: polarization into a pro-inflammatory MSC1 or an immunosuppressive MSC2 phenotype. *PLoS One*. 2010;5(4):e10088.
19. Thery C, Amigorena S, Raposo G, Clayton A. Isolation and characterization of exosomes from cell culture supernatants and biological fluids. *Curr Protoc Cell Biol*. 2006. Chapter 3:Unit 3.22.
20. Cooke KR, Kobzik L, Martin TR, et al. An experimental model of idiopathic pneumonia syndrome after bone marrow transplantation, I: the roles of minor H antigens and endotoxin. *Blood*. 1996;88(8):3230–3239.
21. Koh TJ, DiPietro LA. Inflammation and wound healing: the role of the macrophage. *Expert Rev Mol Med*. 2011;13:e23.
22. Gordon S, Martinez FO. Alternative activation of macrophages: mechanism and functions. *Immunity*. 2010;32(5):593–604.
23. Snyder RJ, Lantis J, Kirsner RS, Shah V, Molyneaux M, Carter MJ. Macrophages: a review of their role in wound healing and their therapeutic use. *Wound Repair Regen*. 2016;24(4):613–629.
24. Phinney DG, Pittenger MF. Concise review: MSC-derived exosomes for cell-free therapy. *Stem Cells*. 2017;35(4):851–858.
25. Katsuda T, Kosaka N, Takeshita F, Ochiya T. The therapeutic potential of mesenchymal stem cell-derived extracellular vesicles. *Proteomics*. 2013;13(10-11):1637–1653.
26. Lai RC, Yeo RW, Lim SK. Mesenchymal stem cell exosomes. *Semin Cell Dev Biol*. 2015;40:82–88.
27. Yu B, Zhang X, Li X. Exosomes derived from mesenchymal stem cells. *Int J Mol Sci*. 2014;15(3):4142–4157.
28. ELA S, Mager I, Breakefield XO, Wood MJ. Extracellular vesicles: biology and emerging therapeutic opportunities. *Nat Rev Drug Discov*. 2013;12(5):347–357.
29. Shah R, Patel T, Freedman JE. Circulating extracellular vesicles in human disease. *N Engl J Med*. 2018;379(10):958–966.
30. Wen S, Dooner M, Cheng Y, et al. Mesenchymal stromal cell-derived extracellular vesicles rescue radiation damage to murine marrow hematopoietic cells. *Leukemia*. 2016;30(11):2221–2231.
31. Ti D, Hao H, Tong C, et al. LPS-preconditioned mesenchymal stromal cells modify macrophage polarization for resolution of chronic inflammation via exosome-shuttled let-7b. *J Transl Med*. 2015;13(1):308.
32. Suffredini AF, Noveck RJ. Human endotoxin administration as an experimental model in drug development. *Clin Pharmacol Ther*. 2014;96(4):418–422.
33. Chow A, Huggins M, Ahmed J, et al. CD169(+) macrophages provide a niche promoting erythropoiesis under homeostasis and stress. *Nat Med*. 2013;19(4):429–436.
34. Jacobsen RN, Perkins AC, Levesque JP. Macrophages and regulation of erythropoiesis. *Curr Opin Hematol*. 2015;22(3):212–219.
35. Heideveld E, van den Akker E. Digesting the role of bone marrow macrophages on hematopoiesis. *Immunobiology*. 2017;222(6):814–822.
36. Ploeger DT, Hosper NA, Schipper M, Koerts JA, de Rond S, Bank RA. Cell plasticity in wound healing: paracrine factors of M1/ M2 polarized macrophages influence the phenotypical state of dermal fibroblasts. *Cell Commun Signal*. 2013;11(1):29.
37. Italiani P, Boraschi D. From monocytes to M1/M2 macrophages: phenotypical vs. functional differentiation. *Front Immunol*. 2014;5:514.
38. Linden J. Molecular approach to adenosine receptors: receptor-mediated mechanisms of tissue protection. *Annu Rev Pharmacol Toxicol*. 2001;41:775–787.